Research Article: Archaeological Science

Detecting traces of invisible Egyptian Blue on a limestone stela fragment with reflection, luminescence, and spectroscopic techniques

Athena Van der Perre[1,*], Dennis Braekmans[2], Vanessa Boschloos[3,4], and Hendrik Hameeuw[1]

[1]KU Leuven, Leuven
[2]Leiden University, Leiden
[3]Ghent University, Ghent
[4]Johannes Gutenberg-Universität Mainz, Mainz

Published: 1st September 2026

Abstract

Many stone artefacts from antiquity—including stelae and statues—were frequently decorated with vivid colours. Today, these have mostly faded or entirely disappeared, being no longer visible to the human eye. This case study explores several non-invasive methods to monitor, detect, and identify the traces of ancient Egyptian pigments on a limestone medium, particularly focusing on Egyptian Blue. The selected object is a fragment of a limestone stela decorated with an incised and coloured offering scene, dating to the early New Kingdom (*ca.* 1550–1292 BCE). The applied methods are reflection photography, visible-induced infrared luminescence (VIL), white light multi-light reflectance (WL MLR), and mobile X-ray fluorescence spectroscopy, both point (pXRF) and mapping (p-μXRF). The applied techniques, which vary in user complexity and user accessibility, substantiate the presence of the Egyptian Blue pigment and others on the relief when used all together, but equally indicate how the methods can be used separately for the same purpose.

Keywords: Egyptian blue, limestone stela, pigments, visible-induced infrared luminescence (VIL), energy dispersive X-ray fluorescence (ED-XRF)

الكشف عن البقايا غير المرئية لصبغة الأزرق المصري على جزءٍ من لوحة جنائزية من الحجر الجيري باستخدام تقنيات الانعكاس، والتألّق، والتحليل الطيفي

الملخص

زُيّنت العديد من القطع الحجرية التي تعود إلى العصور القديمة، بما في ذلك اللوحات الجنائزية والتماثيل، بألوان زاهية. إلا أن معظم هذه الألوان قد تلاشى مع مرور الزمن أو اختفى تمامًا، بحيث لم يعد مرئيًا للعين المجردة. لذا تستعرض هذه الدراسة التطبيقية مجموعةً من التقنيات غير المتلفة لرصد وكشف وتحديد بقايا الأصباغ المصرية القديمة على قطعةٍ من لوحة جنائزية من الحجر الجيري، مع التركيز بصورة خاصة على صبغة الأزرق المصري. حيث يتمثل موضوع الدراسة في كسرة من لوحة جنائزية مصنوعة من الحجر الجيري، ومزخرفة بمشهدٍ للقرابين محفورٍ وملوَّن، ويرجع تاريخها إلى بدايات الدولة الحديثة (حوالي 1550–1292 ق.م). وقد استُخدمت في الدراسة عدة تقنيات، هي: التصوير بالانعكاس، والتألّق بالأشعة تحت الحمراء المستحث بالضوء المرئي (VIL)، وتقنية الانعكاس متعدد الإضاءة باستخدام الضوء الأبيض (WL MLR)، بالإضافة إلى مطيافية التألق بالأشعة السينية المحمولة، سواء في القياسات النقطية (pXRF) أو الخرائطية .(p-µXRF) وتؤكد النتائج أن الجمع بين هذه التقنيات، على الرغم من اختلافها من حيث درجة تعقيد استخدامها وإمكانية تطبيقها،

*Corresponding Author: athena.vanderperre@kuleuven.be

DOI: 10.25365/integ.2026.v5.2

قد أتاح إثبات وجود صبغة الأزرق المصري وغيرها من الأصباغ على سطح النقش البارز. كما تُظهر الدراسة أيضًا إمكانية استخدام كل تقنية من هذه التقنيات بصورة مستقلة لتحقيق الغرض ذاته.

الكلمات الدالة الأزرق المصري , لوحة جنائزية من الحجر الجيري , الأصباغ , التألّق بالأشعة تحت الحمراء المستحث بالضوء المرئي (VIL) , مطيافية التألق بالأشعة السينية المشتتة للطاقة (ED-XRF)

1 Introduction

Art-technical and material studies on heritage objects, and certainly those in museum collections, often only authorise non-touch and non-destructive examinations. This study explores several non-invasive methods to detect, identify, and monitor an object's materiality, in particular on a limestone medium. Limestone, an easily workable sedimentary rock widespread in the Nile Valley and Eastern and Western Egyptian deserts, was primarily used as a building material, but also abundantly for carved objects such as stelae, statues, and reliefs (Aston et al., 2000: 40–42). In some cases, a layer of lime is applied before painting, while in others, the paint goes directly onto the finished stone surface. For the latter, the high porosity of limestone allows for penetration of pigments, which, depending on used binders, ground, and environmental conditions, may improve their preservation. This study examines how Visible-induced Luminescence (VIL) and X-Ray Fluorescence (XRF) techniques, separately and combined, can contribute to detecting faded or visually indiscernible traces of Egyptian Blue. It centres on the examination of a fragment of an ancient Egyptian limestone slab, measuring 95×95×38 mm (KU Leuven, ancient inv. N°563, ARO000004). The original surface was finished straight and flat—fine chisel marks are visible—and was decorated with an offering scene in shallow raised relief. The relief fragment is the lower right part of a limestone offering stela; the left and upper edges are lost. The stela, an example of an object category common in Egyptian archaeology, was originally decorated in vivid colours. The back of the fragment is roughly shaped.

The scene on the front depicts a male figure, whose skin still bears traces of red pigment, standing in front of an offering table (Figure 1). The man faces left and raises his right hand. He wears a knee-length short kilt with a long over-kilt and a plain, rounded collar. In his left hand, he holds a folded cloth. Above his right hand, the remnants of two incised hieroglyphs are visible, *ḫpr* (𓆣, Gardiner L1) and *r* (𓂋, Gardiner D21). The location of the hieroglyphs suggests that these are part of the name of the depicted person. The table is piled with goods, the bottom layer counts two round loaves of bread, with an oblong loaf in between. Underneath the table, a beer jar on a stand is depicted near the standing figure. The outlines of a second jar are traced on the other side of the table. On the right side, part of the frame surrounding the scene is still visible. The background was originally covered in a yellow pigment. Based on the iconography, the stela dates to the early New Kingdom, *ca.* 1550–1292 bce (cf. Oriental Institute E11455 in Bandy, 2020, Louvre E17402 in Vandier, 1951: 63, Louvre E20237 in Málek, 2012: 164–165).

The provenance of the archaeological object cannot be determined with certainty. On the right side of the object, a note in ink mentions 'Karnak'. However, it remains uncertain whether this refers to the location where the object was discovered or where it was acquired. A round label next to it identifies the object as '563'. This type of label is found on many objects known to have been part of the university's collections of the 'Museum voor Oosterse Oudheden' / 'Musée Oriental' / 'Museum Egyptische en Voor-Aziatische Archeologie', which was installed during the Interbellum (i.e. from 1927 until it was heavily damaged during bombing raids in 1944) on the second floor of the University Hall in Leuven (Danckers & Van den Driessche, 2022: 56, 61–62). The use of this label format confirms that the object was registered in the collection at some point in this period, between 1927 and 1944. Furthermore, the stela appears under the same inventory number in the archival documents on the division of the collection, drafted on 2 May 1974, when half of the collection was moved to the University of Louvain-la-Neuve.

On the surface of the stela, remnants of red and yellow pigments are still visible with the naked eye. The subject matter suggests that certain details, such as the rounded collar of the man, could originally be coloured blue, though remnants of a blue pigment are no longer visible. Therefore, this limestone fragment was selected to examine, non-invasively, the presence of pigments with a selection of visualisation and analytical methods.

2 State-of-the-art

Combining reflectance photographic representations with luminescence and spectroscopic techniques and/or other technical and analytical research methods to study and understand the (artistic) materiality of archaeological finds is a well-trodden path exemplified by a countless number of published studies. Focusing first on the methods used in this contribution, the use of Multi-Light Reflectance (or Reflectance Transformation Imaging) techniques has been widely explored and positively evaluated for the documentation and understanding of surface topography, tool marks, and materiality (Piquette, 2016; Serotta, 2023; Hameeuw et al., 2023). The same applies for VIL, that has been demonstrated both outside Egyptian archaeology and art-technical studies, such as for the Parthenon sculptures (Verri et al., 2023), Neo-Assyrian gypsum reliefs (Thavapalan et al., 2016) and more specifically on a variety of ancient Egyptian objects and monuments, among many see Wiseman et al. (2023) and Dyer and Newman (2020). Limestone media have been examined with analytical methods in a combination of non-destructive techniques such as multispectral imaging and XRF, and destructive techniques such as laser ablation and micro X-ray powder diffraction (see Hedegaard et al., 2019; Cavaleri et al., 2021; Ramadan et al., 2022). On a larger scale, analytical applications are diverse, with research teams often applying a wide range of available methods, as shown in these studies on Roman mummy portraits: Salvant et al. (2018) and Radpour et al. (2022). In recent years, the use of chemical imaging techniques for the study of polychrome objects and surfaces has seen a steep rise. XRF-mapping was used to investigate *in situ* wall paintings (on plastered limestone surfaces) in the Theban necropolis in combination with photography (Martinez et al., 2023), showing the potential for the technique in the field. The combination of Reflectance Imaging Spectroscopy and XRF was evaluated, equally on wall paintings, in 2018 (Alfeld et al., 2018). In similar rock tomb conditions Vandenabeele et al. (2009) conducted an archaeometrical survey combining photographic VIS and UV techniques, XRF and various spectrometry and Raman spectroscopy techniques; equally, Hussein Marey and Papadopoulou (2013) applied an extensive range of techniques to analyse pigments in tomb wall paintings. These are examples of high-profile multi-modal efforts, requiring extensive multi-disciplinary teams. For the study of the limestone stela discussed in this contribution, a targeted selection of mid-end and high-end visualisation and analytical techniques was applied, aimed specifically at redetecting pigments that are no longer visible with the naked eye and their relation to the engraved offering scene. The research infrastructure is also characterised by its full portability, which allows for on-site analysis.

3 Methodology

The applied methods are reflection photography, visible-induced infrared luminescence (VIL), white light multi-light reflectance (WL MLR), and X-ray fluorescence elemental analysis, both point (pXRF) and mapping (p-μXRF). The chemical elemental XRF examinations are assessed in relation to the visible appearance of the relief as registered with the colour calibrated reflection still image. The relief was also examined using the White Light Multi-Light Reflectance (WL MLR) technique to elaborate the surface topography, reveal tool-marks and damages, and make an abstraction from post-production discolourations (Figure 1). Digital microscopy was performed using a Dino-Lite (Model AD4113T, with onboard UV and external white light). As the results did not reveal any pigmentation beyond what was already visible to the naked eye—and provided no added value within the context of this study relative to the high-resolution reflection and multi-light reflectance images—this data is not discussed further below. A combined use of the applied techniques, which vary in user complexity and user accessibility, allows the detection of the Egyptian Blue pigment on the surface, but this paper also examines to which extent the various techniques can be used separately for this purpose.

3.1 Reflection photography

Reflection still image with a Nikon D850 and a Nikon AF-S Micro-Nikkor 60 mm f/2.8G ED lens. Recording and (colour) calibration according to FADGI guidelines (ISO 19264) and written in colour space eciRGB v2. Capture settings are aperture: f11, shutter speed: 1/125 and ISO: 100. This digital image is used for visual comparison and computational assessment of detected colours. Estimated acquisition and processing time: 10 min.[1]

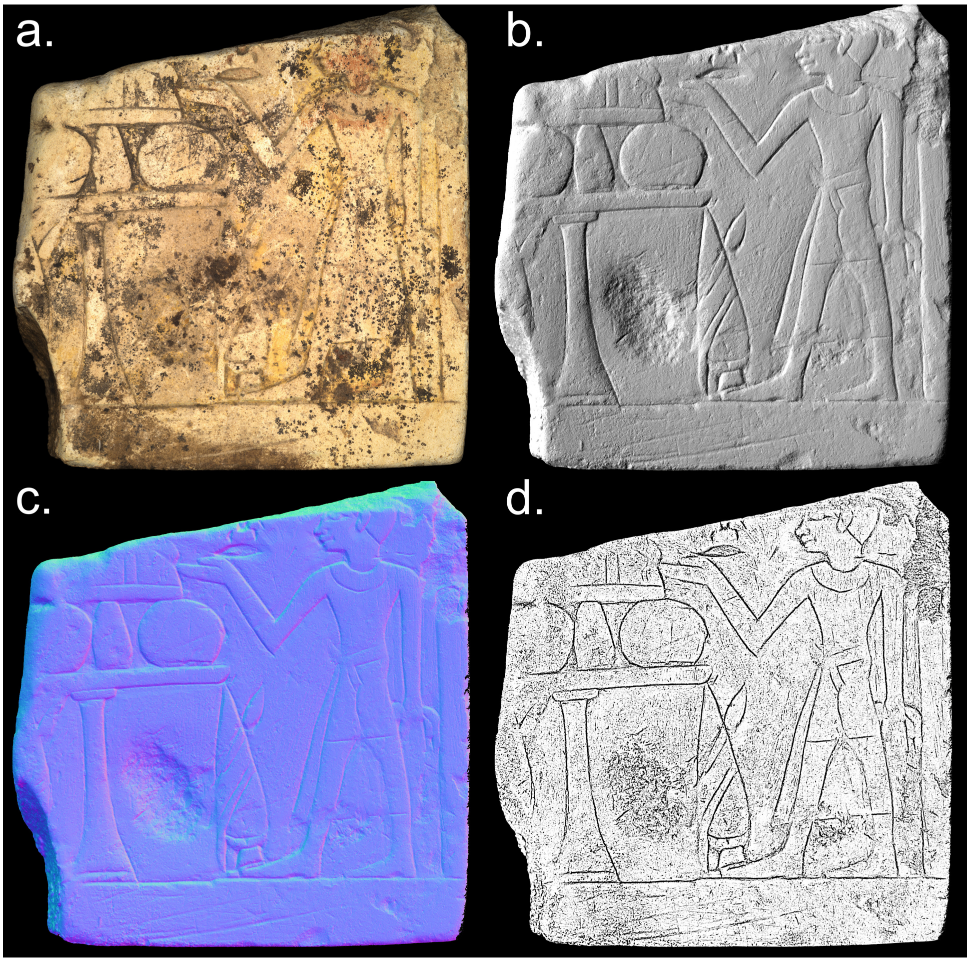

Fig. 1: Multi-Light reflectance renderings in Pixel+ viewer. a: uncalibrated colour in visual style "ambient"; b: visual style "shaded"; c: visual style "normal"; d: visual style "sketch1".

3.2 VIL

Luminescence image obtained with a Phase One IQ4 150MP Achromatic (Sony CMOS-BSI light sensor) and Schneider Kreuznach 120mm LS f/4.0 Macro lens. The applied Infrared (IR) long pass filter is a Schott Glass RG850. Light emitting sources are narrow band LEDs with peak at 640 nm, illuminated from two sides, 35°

[1]This, similar for all other applied assessment techniques in this study, does not include the setup of the system. It estimates the standard acquisition and processing time to obtain a final dataset, on which the assessment can be performed.

angles towards the middle of the object.[2] Capture settings are aperture: f16, shutter speed: 2 min 30 sec, ISO: 200 with enhanced contrast. The object was exposed to the emitting source, and only infrared luminescence that passed through the IR filter was detected. Estimated acquisition and processing time: 5 min.

3.3 WL MLR

Relightable model, including reflectance (albedo) and surface orientations (normal) data, obtained with KU Leuven–VIEW White Light Microdome (VAN DER PERRE et al., 2016). Capture settings are aperture f11, shutter speed 80 ms. Digital model reveals the detailed surface topography and contextualises the engravings with the applied remnants of pigments. Estimated acquisition and processing time: 15 min.

3.4 pXRF

Measurements are performed with a Bruker Tracer III-SD, operating under 40kV, 10μA for 30 seconds in air using no filter, consisting of a Rh anode X-ray tube and a Peltier-cooled Silicon Drift Detector (~145 eV at Mn Kα). Spot size of the different areas is approximately 10 mm². Net peak areas were calculated for the different elements through proprietary Bruker ARTAX software. Estimated acquisition time is 30 seconds (excluding setting up the instrument), evaluating and calculating net peak areas of a dataset for the different elements has an estimated processing time of 1 h.

3.5 p-μXRF-mapping

Point measurements mapped with a Bruker Elio, operating under 50kV, 40μA per point for 1 second in air using no filter, consisting of a Rh anode X-ray tube with a Silicon Drift Detector (~130 eV at Mn Kα). Mapped area is 99×99 mm, spot size 1000 μm, interval 1000 μm. The converted pixel maps plot the distribution per chemical element, revealing concentrations of particular elements, whether or not allowing the positive identification of the remnants of applied materials. The maps were produced with the Esprit Reveal software (v2.6.0.1028) proprietary settings plotting the counts (i.e. 'normalize to zero peak'). Estimated acquisition and processing time: 6h, post processing to produce chemical maps: 1 h.

4 Results and discussion

4.1 Egyptian Blue

Egyptian Blue is a synthetically manufactured blue pigment (KOVALEV et al., 2023), i.e. a calcium copper silicate ($CaCuSi_4O_{10}$), and in ancient Egypt already in use by the end of the Predynastic period (CORCORAN, 2016). The silica-rich limestone medium of the relief, $CaCO_3$ (Figure 4 and Figure 6) makes the unique chemical identifier for the Egyptian Blue to be copper. When visually inspecting the offering stela (with the naked eye or by colour-calibrated reflection photography, *idem* microscopic inspection), no areas or spots that appear blue can be detected (see Figure 2). Only near-neutral grey areas or spots are observed, which could hint to faded, originally blue coloured materials, but equally coincide with most of the manganese (Mn) rich zones on the relief's surface (see Figure 6). Therefore, based on the visual inspection of the stela alone, the presence of Egyptian Blue cannot be corroborated.

As an ancient pigment, Egyptian Blue has a unique luminescence property (VERRI, 2009b; VERRI, 2009a; CHIARI, 2018). To reveal its presence, the visible-induced infrared luminescence (VIL) method was applied

[2] For all technical specs on the applied systems, see https://doi.org/10.5281/zenodo.7410238.

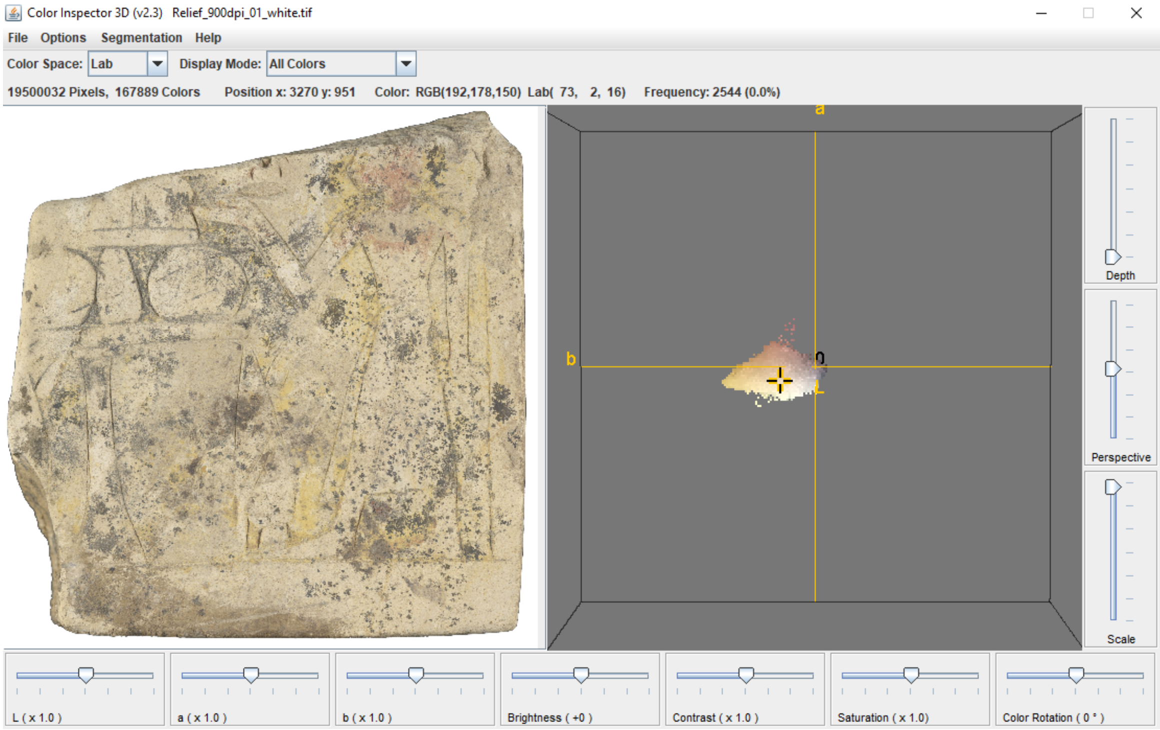

Fig. 2: Plotted L*a*b* values of the colour calibrated (FADGI) relief surface with remnants of pigments, revealing virtually no blue (–b) on the surface (ImageJ Color Inspector 3D v2.3).

on the offering stela. When irradiated with white light (within the range 400–700 nm) the copper ions (Cu^{2+}) in Egyptian Blue have a very strong luminescence effect in IR. The materials that luminesced registered as bright in the resulting image (see Figure 3). At least three distinct features on the relief fragment appear to have been coloured in Egyptian Blue: the standing figure's collar, the remaining section of the stela's frame just behind the figure, and the support of the offering table.

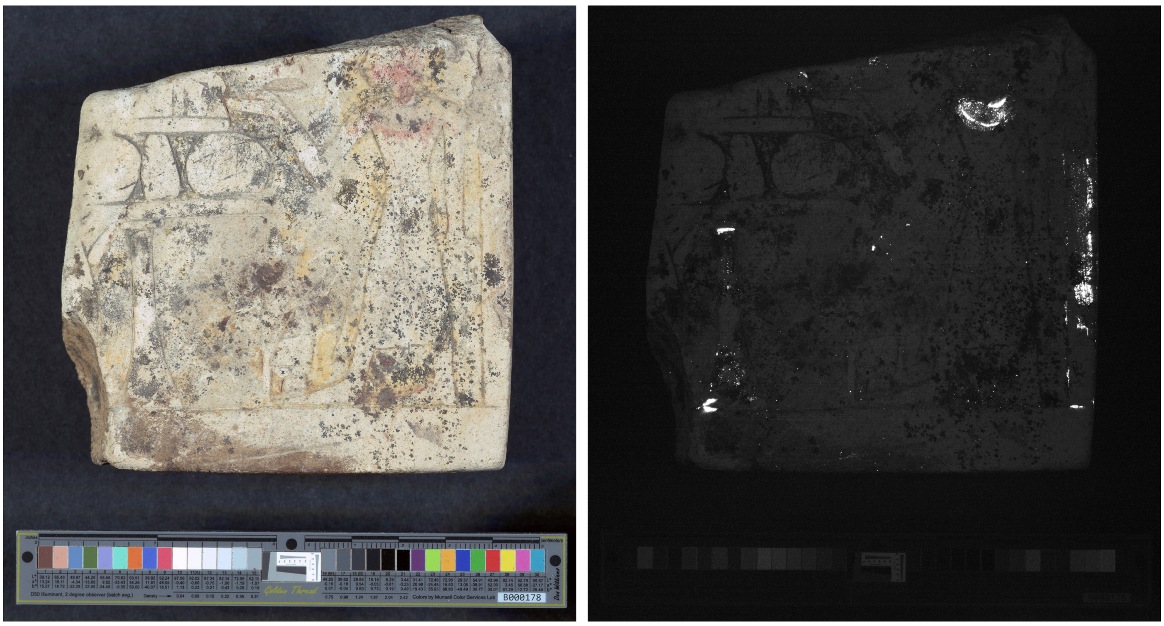

Fig. 3: Left: colour-calibrated RGB image. Right: visible-induced infrared luminescence (VIL).

The VIL test provides the most straightforward, clear, and refined evidence for the presence of Egyptian Blue, but this method is not 100% conclusive when it is not combined with a technique that provides insight into the chemical composition of an examined area or spot. Cadmium-based (yellow/orange/red) and zinc-oxide (white) pigments, not used in antiquity, luminesce in a similar manner as Egyptian Blue and would also show up with a VIL test (Thoury et al., 2011; Verri & Saunders, 2014; Daveri et al., 2016). Therefore, when modern, but already faded restorations using these pigments would have been applied on the original surface, this might lead to misinterpretations. Since the stela's object life is not known prior to its entry into the KU Leuven collection, these zones must be analysed further by determining the chemical composition of the pigment remains, in order to conclusively identify and validate the pigmented areas. By using a portable X-ray fluorescence (pXRF) system, individual point spots are measured, focusing on a qualitative analysis into the relative presence and absence of elements that can be important for pigment identification. In this particular case, the analysis determines qualitatively whether enrichments in e.g. Cu can be detected in areas of interest with a potential pigment presence that might further indicate the presence of Egyptian Blue (Tite et al., 1987). As a comparative approach several different areas were targeted: spots on the head, collar, as well as on the yellow-coloured background field. The collected spectra were assessed for depletions and enrichments between the different attested elements. Figure 4 shows the different indicative spectra for these head, collar, abdomen, and background areas. All these spectra show consistent patterns with only divergent intensities for Cu, Fe, and As. The area of the abdomen does not yield significant elemental peaks other than Ca and Fe, which are consistent with most of the other spectra, and thus can be considered a measurement of the limestone background. The yellow background has a clear enrichment in Fe (cf. discussion on other pigments below). The head is characterised by an increased trace presence of arsenic whereas the collar area has a clear Cu peak present (cf. detail Figure 5). Calculated net peak areas of these spectra using a Bayesian deconvolution approach are provided in Table 1.

Tab. 1: Net peak areas of the X-ray fluorescence analysis. Overall consistent aside an approximate double amount of Cu that is present in the area of the collar.

	As Kα	Ca Kα	Cu Kα	Fe Kα	K Kα	Mn Kα	Ni Kα	Pb Lα	S Kα	Sr Kα	Ti Kα
Abdomen (limestone)	530	256549	3565	128165	1387	9870	3210	1045	159	21370	1851
Collar	1363	300556	7935	127073	1482	10360	3268	1064	566	22989	2442
Head (red)	3014	317957	3848	121136	1194	11205	3872	1257	373	23081	2179
Background field (yellow)	1362	243885	3950	234799	1627	4489	3415	821	263	23157	5030

The more time consuming and more expensive p-μXRF-mapping technique delivers the same insights with a vast amount of data supporting the identification of varied materials and pigments. It has the ability to provide mapped invisible information on remnants of faded materials on limestone. As for VIL, the technique gives spatial information on the entire examined surface. As in the case of the no longer visible remnants of Egyptian Blue, single point measurements risk overlooking these areas. The chemical elemental map of copper (Figure 6: Cu) shows high concentrations of Cu on the same graphical features (i.e. collar, offering table and frame) as were highlighted by the VIL test.

Unfortunately, copper is not only a unique chemical identifier for Egyptian Blue, but also for certain green pigments, e.g. malachite. While the use of solely XRF could deliver a false identification for the pigment, the combination of the XRF methods with VIL, as already mentioned above, ensures that the identification as Egyptian Blue is conclusive.

To conclude, Egyptian Blue is found on both the standing male figure's collar and the offering table. Furthermore, the pigment is also detected in the stela's surrounding frame (Figure 7). This is consistent with the artistic and cultural practices of the time (cf. Louvre E8401 in Málek, 2012: 162).

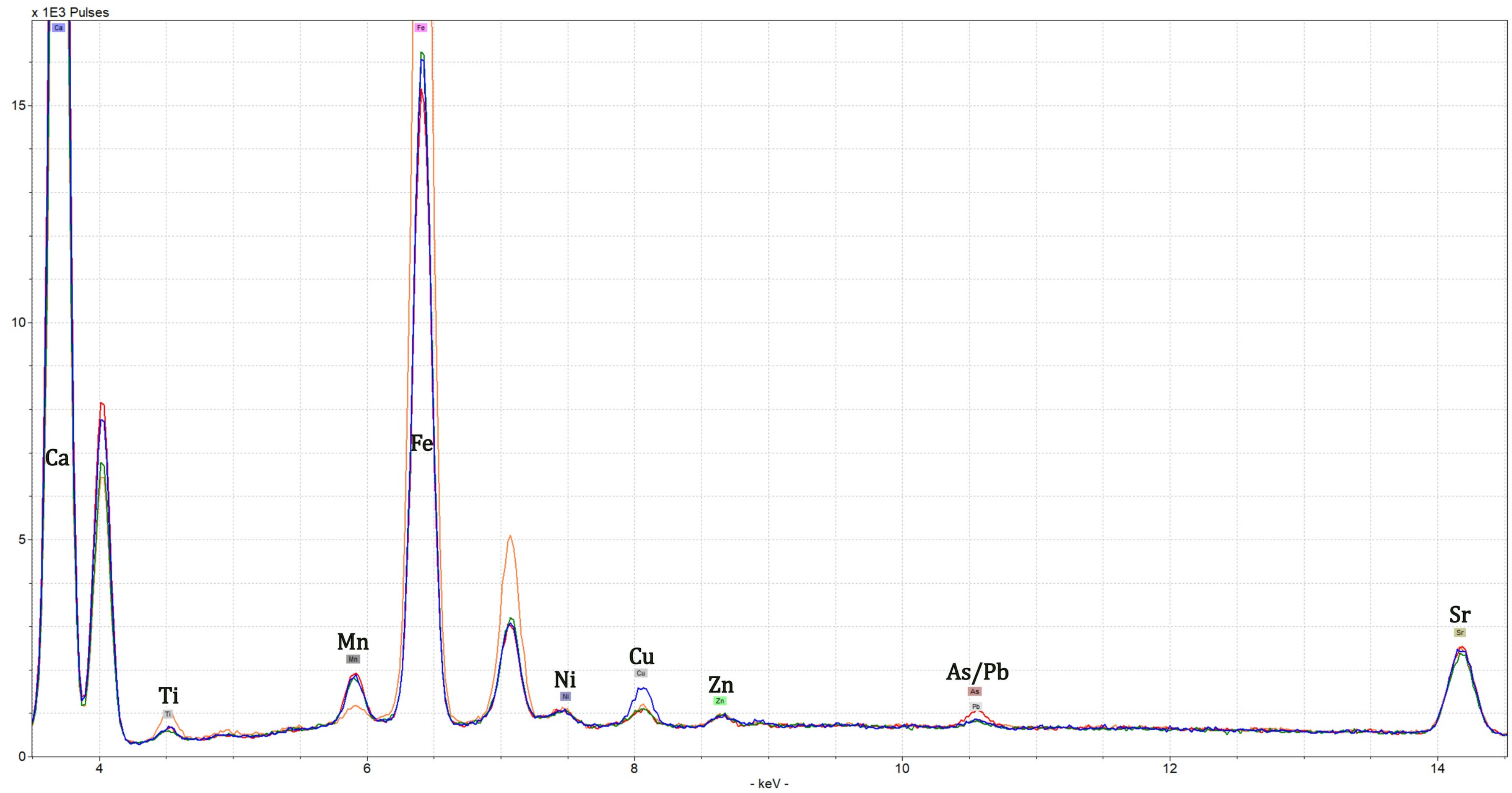

Fig. 4: pXRF-point measurements: (1) green spectrum = middle of the abdomen of the figure (i.e. zone without visible pigment, thus limestone medium only); (2) orange = yellow coloured background zone at the left of object; (3) red = head of the figure (i.e. zone with visible red pigment); (4) blue = middle of collar of the figure (i.e. zone without visible pigment), with enrichment in copper.

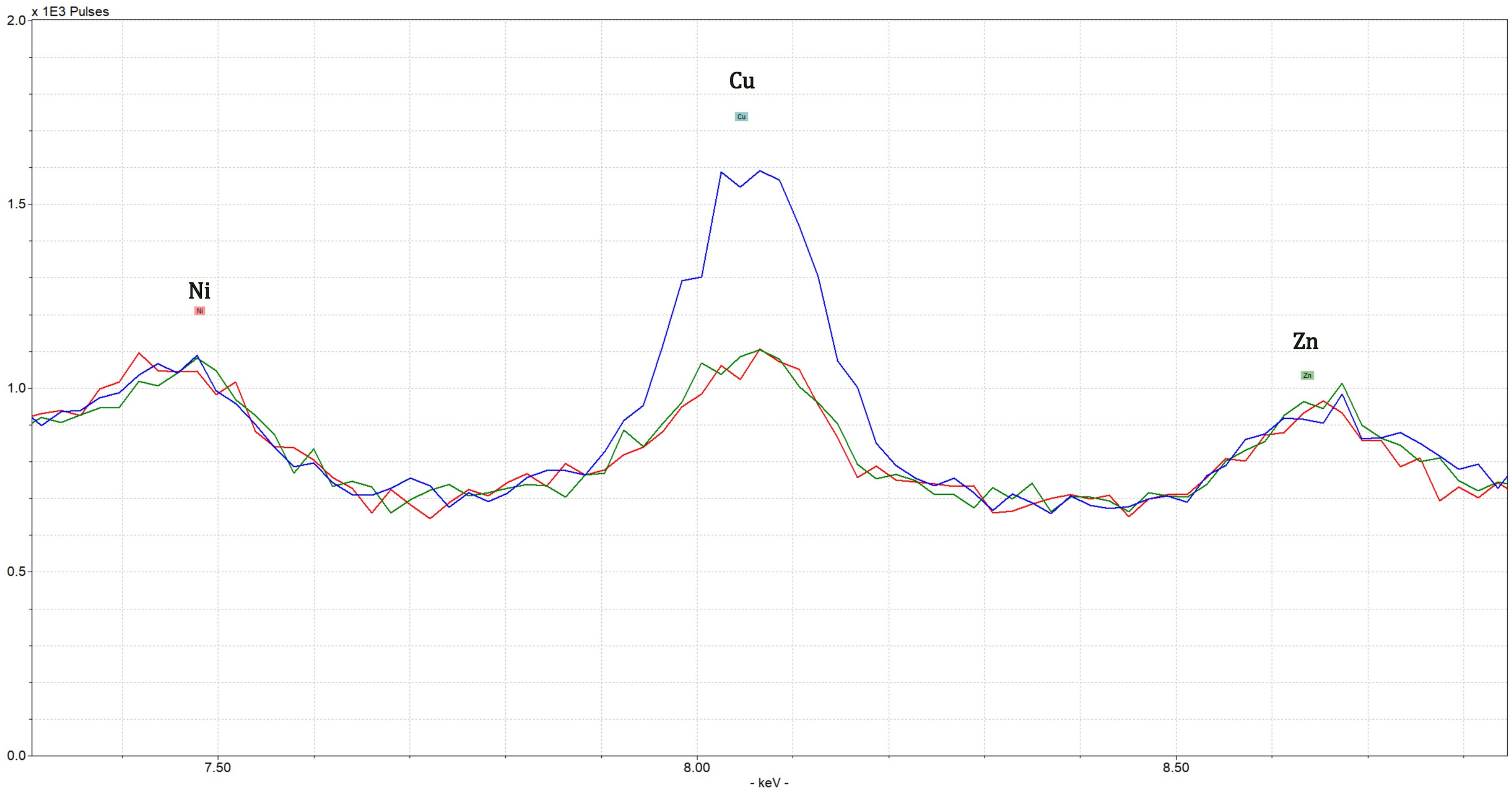

Fig. 5: pXRF-point measurements, detail of collar area (blue) versus abdomen and head areas (green and red). In the blue spectrum a clear enrichment of Cu is detected.

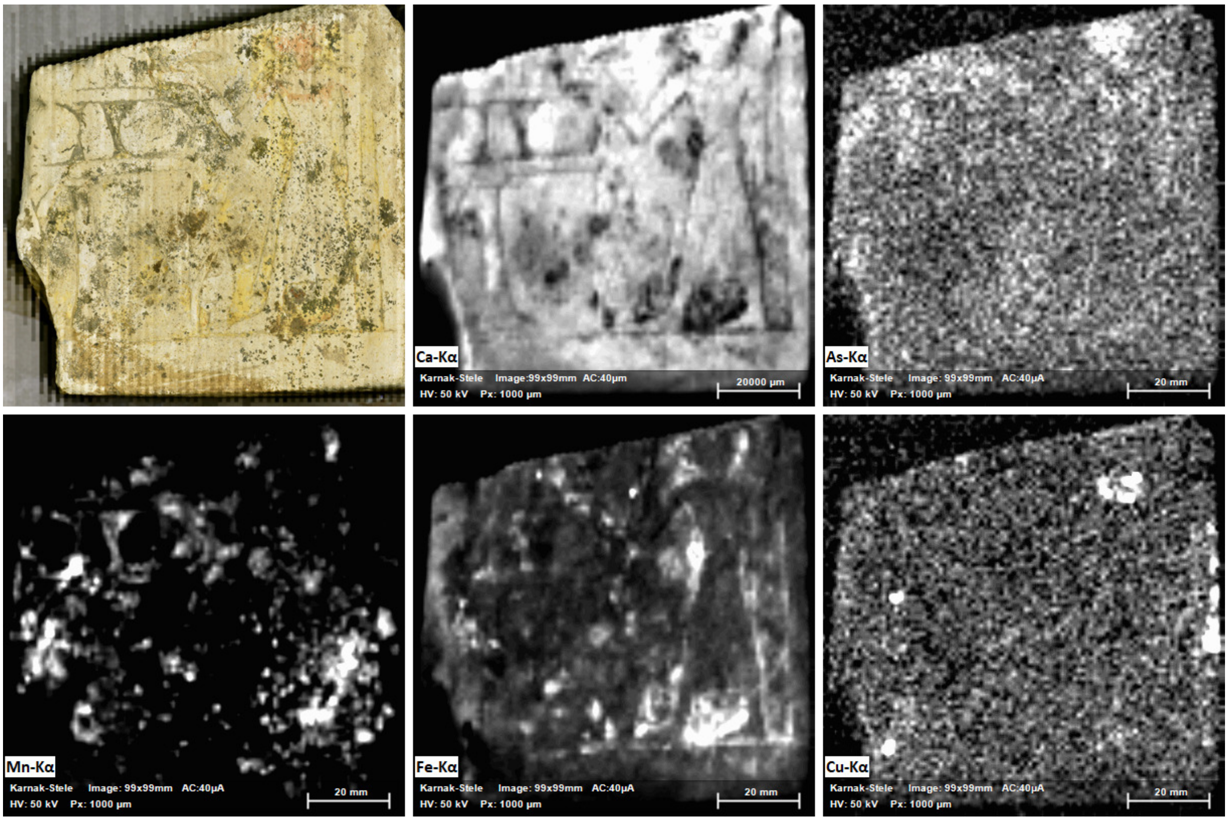

Fig. 6: p-μXRF-mapping: visual and a selection of elemental maps of the entire front of the stela, for Ca, As, Mn, Fe, and Cu (all Kα).

4.2 Yellow and red pigments

The background field of the engraved relief was covered with a yellow, slightly powdery colourant. It is still visible in various areas across the surface and contains high levels of iron (Fe) correlated with an enrichment in titanium (Ti) (see pXRF, Table 1, and p-μXRF-mapping, Figure 6). This background reveals no other chemical markers, deviating from the limestone medium, and can therefore be determined as a yellow ochre pigment, the most commonly used yellow pigment during the Pharaonic period (LEE & QUIRKE, 2000: 115). The practice of using yellow pigments for the background of pictorial scenes is frequently attested at the beginning of the New Kingdom (cf. Oriental Institute E11455 in BANDY, 2020, Louvre E17402 in VANDIER, 1951: 63, Louvre E20237 in MÁLEK, 2012: 164–165, and COLINART, 2001).

Remnants of a solid red pigment are clear on the male figure's bare skin and on the remaining incised hieroglyphs. However, as the pXRF and p-μXRF-mapping results lack iron (Fe) for these spots (Figure 4 and Figure 6), the pigment cannot be identified as the commonly used red ochre. As a chemical marker, deviating from the limestone medium, only a minor arsenic enrichment (As) is attested based on the Bayesian deconvolution of the obtained pXRF spectra, see Table 1. Based on this information, the red pigment can therefore most probably be identified as (para)realgar (As_4S_4), which became more common as red colourant from the New Kingdom onwards (SCOTT, 2016: 193; MIDDLETON & HUMPHREY, 2001). Nevertheless, since no clear indications for sulphur (S) are found, this particular pigment might also be organic in nature, and its identification should therefore be regarded as provisional.

Fig. 7: Left: colour-calibrated RGB image. Right: 3D model with virtual estimation of the original artistic colour scheme.

5 Conclusion

The reflection, luminescence, and spectroscopic techniques—MLR, VIL imaging, and XRF analysis—are powerful, complementary techniques significantly advancing the study of deteriorated polychrome objects and surfaces and the identification of ancient pigments. In this study, those abilities have been successfully used for the complementary detection of visually completely vanished Egyptian Blue and for analysing the visual remnants of an iron-containing yellow ochre pigment and an iron-lacking red, presumably realgar pigment. The applied techniques enrich the visual and material understanding of ancient Egyptian art, but also contribute to broader questions about its condition and conservation.

The variety of the applied assessment techniques all contribute to the full documentation of the fragment, to a better understanding of the surface characteristics, and to a positive identification of the original presence of Egyptian Blue on the stela, now no longer visually detectable. In addition, as little is known on the stela's object life, this identification of Egyptian Blue makes a compelling argument to confirm the authenticity of the artefact.

The VIL, pXRF and p-μXRF-mapping results all lead to the same conclusions. When used independently from each other, they are each effective to hint at the presence of Egyptian Blue when applied on a limestone medium. The VIL test still provides the most straightforward, clear and refined evidence for Egyptian Blue. This method, however, is not always conclusive when it is not combined with a technique that provides insight into the chemical composition of an examined area or spot (cf. modern cadmium-based or zinc-oxide pigments). The present study methodologically demonstrated that even a single, well-targeted XRF point measurement immediately provides a definitive answer. On the other hand, the pXRF data on its own could still lead to other pigments, such as the Cu-holding green pigment malachite. The combination of both non-invasive techniques (VIL and pXRF), when available, is therefore the preferred method for the positive identification of these invisible traces as Egyptian Blue. It remains to be clarified to what extent this methodology gives consistently equal results on the medium limestone. Over time and space the finished product of the pigment shows variations, i.e. dependent on the specific characteristics and processing of raw materials, the exact mixture of raw materials, the firing (pyro-chemical) process, and the final processing at the artistic workshop applying the pigment, as discussed by KOVALEV et al. (2023).

In addition, the combination of the techniques allows an attempt at partly reconstructing the limestone stela's original artistic colouring scheme (Figure 7). The damaged area next to the offering table still shows remains of the yellow pigment, confirming that this damage was already present before the final pigment layer was applied. On the 3D model rendered with the WL MLR data, the three attested pigments have been colourised in all zones on which they were originally applied. The zones for which no clear pigment traces could be found, were left blank.

6 Acknowledgments

This study has been supported by the KU Leuven Core Facility VIEW and the SIG.NILE consortium (active at the universities of Leuven, Leiden, and Ghent).

References

ALFELD, M., PEDETTI, S., MARTINEZ, P., & WALTER, P. (2018). Joint data treatment for Vis–NIR reflectance imaging spectroscopy and XRF imaging acquired in the Theban Necropolis in Egypt by data fusion and t-SNE. *Comptes Rendus Physique*, *19*(7), 625–635.

ASTON, B., HARRELL, J., & SHAW, I. (2000). Stone. In P. NICHOLSON & I. SHAW (Eds.), *Ancient Egyptian materials and technology* (5–77). Cambridge: Cambridge University Press.

BANDY, K. E. (2020). A Family of Lector-Priests at Edfu: Oriental Institute Stela E11455 and the Ib Family during the Early Eighteenth Dynasty. *Journal of the American Research Center in Egypt*, *56*, 47–69.

CAVALERI, T., LEGNAIOLI, S., LOZAR, F., COMINA, C., POOLE, F., PELOSI, C., SPOLADORE, A., CASTELLI, D., & PALLESCHI, V. (2021). A Multi-Analytical Study of an Ancient Egyptian Limestone Stele for Knowledge and Conservation Purposes: Recovering Hieroglyphs and Figurative Details by Image Analysis. *Heritage*, *4*(3), 1193–1207.

CHIARI, G. (2018). Photoluminescence of Egyptian Blue. In V. LÓPEZ (Ed.), *The Encyclopedia of Archaeological Sciences*. Chichester: Wiley Blackwell.

COLINART, S. (2001). Analysis of inorganic yellow colour in Egyptian painting. In W. V. DAVIES (Ed.), *Colour and Painting in Ancient Egypt* (1–4). London: British Museum Press.

CORCORAN, L. H. (2016). The color blue as an 'Animator' in ancient Egyptian art. In R. B. GOLDMAN (Ed.), *Essays in Global Color History* (41–63). Piscataway: Gorgias Press.

DANCKERS, J., & VAN DEN DRIESSCHE, B. (2022). *Boegbeeld in de kelder. Een geschiedenis van de archeologische collectie van de KU Leuven*. Leuven: Universitaire Pers Leuven.

DAVERI, A., VAGNINI, M., NUCERA, F., AZZARELLI, M., ROMANI, A., & CLEMENTI, C. (2016). Visible-induced luminescence imaging: A user-friendly method based on a system of interchangeable and tunable LED light sources. *Microchemical Journal*, *125*, 130–141.

DYER, J., & NEWMAN, N. (2020). Multispectral Imaging Techniques Applied to the Study of Romano-Egyptian Funerary Portraits at the British Museum. In M. SVOBODA & C. R. CARTWRIGHT (Eds.), *Mummy Portraits of Roman Egypt: Emerging Research from the APPEAR Project* (54–67). Los Angeles: J. Paul Getty Trust.

Hameeuw, H., Van der Perre, A., & Boschloos, V. (2023). Interactive 2D and Multispectral Imaging on the Crossroads of Archaeology, Egyptology and Assyriology. In V. Bigot Juloux, A. Di Ludovico & S. Matskevich (Eds.), *The Ancient World Goes Digital* (72–111). Leiden: Brill. ↗.

Hedegaard, S. B., Delbey, T., Brøns, C., & Rasmussen, K. L. (2019). Painting the Palace of Apries II: ancient pigments of the reliefs from the Palace of Apries, Lower Egypt. *Heritage Science*, *7*, 54. ↗.

Hussein Marey, M., & Papadopoulou, L. (2013). Archaeometric Analysis of Pigments from the Tomb of Nakht-Djehuty (TT189). *ArcheoSciences*, *37*, 19–33. ↗.

Kovalev, I., Rodler, A. S., Brøns, C., & Rehren, T. (2023). Making and working Egyptian blue – a review of the archaeological evidence. *Journal of Archaeological Science*, *153*, 105772. ↗.

Lee, L., & Quirke, S. (2000). Painting materials. In P. T. Nicholson & I. Shaw (Eds.), *Ancient Egyptian Materials and Technology* (104–120). Cambridge: Cambridge University Press.

Málek, J. (2012). *Topographical bibliography of ancient Egyptian hieroglyphic texts, reliefs, and paintings 8: Objects of Provenance Unknown.* Oxford: Griffith Institute.

Martinez, P., Alfeld, M., Defeyt, C., Elleithy, H., et al. (2023). Hidden mysteries in ancient Egyptian paintings from the Theban Necropolis observed by in-situ XRF mapping. *PLOS ONE*, *18*(7), e0287647. ↗.

Middleton, A., & Humphrey, S. (2001). Pigments on Some Middle Kingdom Coffins. In W. V. Davies (Ed.), *Colour and Painting in Ancient Egypt* (10–16). London: British Museum Press.

Piquette, K. E. (2016). Documenting early Egyptian imagery: analysing past technologies and materialities with the aid of Reflectance Transformation Imaging (RTI). In G. Graff & A. Jiménez Serrano (Eds.), *Préhistoires de l'écriture: iconographie, pratiques graphiques et émergence de l'écrit dans l'Égypte prédynastique* (Préhistoires de la Méditerranée; 87–112). Aix-en-Provence: Presses Universitaires de Provence.

Radpour, R., Gates, G. A., Kakoulli, I., & Delaney, J. K. (2022). Identification and mapping of ancient pigments in a Roman Egyptian funerary portrait by application of reflectance and luminescence imaging spectroscopy. *Heritage Science*, *10*, 8. ↗.

Ramadan, S., Mahgoub, G., ElHagrassy, M. S., A. F. Abdel-Aziz, & Mertah, E. (2022). Investigation and Characterization of Two Painted Limestone Stelae, Egyptian Museum, Cairo, Egypt. *Egyptian Journal of Chemistry*, *65*(8), 85–96.

Salvant, J., Williams, J., Ganio, M., Casadio, F., Daher, C., Sutherland, K., Monico, L., Vanmeert, F., De Meyer, S., Janssens, K., Cartwright, C., & Walton, M. (2018). A Roman Egyptian painting workshop: technical investigation of the portraits from Tebtunis, Egypt. *Archaeometry*, *60*(4), 815–833. ↗.

Scott, D. A. (2016). A review of ancient Egyptian pigments and cosmetics. *Studies in Conservation*, *61*(4), 185–202. ↗.

Serotta, A. (2023). Reading Tool Marks on Egyptian Stone Sculpture. *Rivista del Museo Egizio*, *7*, 69–92. ↗.

Thavapalan, S., Stenger, J., & Snow, C. (2016). Color and Meaning in Ancient Mesopotamia: The Case of Egyptian Blue. *Zeitschrift für Assyriologie und vorderasiatische Archäologie*, *106*(2), 198–214. ↗.

Thoury, M., Delaney, J. K., de la Rie, E. R., Palmer, M., Morales, K., & Krueger, J. (2011). Near-Infrared Luminescence of Cadmium Pigments: In situ Identification and Mapping in Paintings. *Applied Spectroscopy*, *65*(8), 939–951. ↗.

TITE, M. S., BIMSON, M., & COWELL, M. R. (1987). The technology of Egyptian blue. In M. BIMSON & I. C. FREESTONE (Eds.), *Early Vitreous Materials* (British Museum Occasional Paper; 39–46). London: British Museum Press.

VAN DER PERRE, A., HAMEEUW, H., BOSCHLOOS, V., DELVAUX, L., PROESMANS, M., VANDERMEULEN, B., VAN GOOL, L., & WATTEEUW, L. (2016). Towards a Combined Use of IR, UV and 3D-Imaging for the Study of Small Inscribed and Illuminated Artefacts. In P. M. HOMEM (Ed.), *Lights On … Cultural Heritage and Museums!* (163–192). Porto: LabCR & FLUP.

VANDENABEELE, P., GARCIA-MORENO, R., MATHIS, F., LETERME, K., VAN ELSLANDE, E., HOCQUET, F.-P., RAKKAA, S., LABOURY, D., MOENS, L., STRIVAY, D., & HARTWIG, M. (2009). Multi-disciplinary investigation of the tomb of Menna (TT69), Theban Necropolis, Egypt. *Spectrochimica Acta Part A: Molecular and Biomolecular Spectroscopy*, *73*(3), 546–552. ↗.

VANDIER, J. (1951). Chronique de l'art ancien et moderne. *La Revue des arts*, *1*, 62–64.

VERRI, G. (2009a). The Application of Visible-Induced Luminescence Imaging to the Examination of Museum Objects [Munich, 17–18 June 2009]. *Proceedings of SPIE: SPIE Europe – Optical Metrology. O3A: Optics for Arts, Architecture, and Archaeology II*, *7391*. ↗.

VERRI, G. (2009b). The spatially resolved characterization of Egyptian blue, Han blue and Han purple by photo-induced luminescence digital imaging. *Analytical and Bioanalytical Chemistry*, *394*, 1011–1021.

VERRI, G., GRANGER-TAYLOR, H., JENKINS, I., SWEEK, T., WEGLOWSKA, K., & WOOTTON, W. T. (2023). The goddess' new clothes: the carving and polychromy of the Parthenon Sculptures. *Antiquity*, *97*(395), 1173–1192. ↗.

VERRI, G., & SAUNDERS, D. (2014). Xenon flash for reflectance and luminescence (multispectral) imaging in cultural heritage applications. *British Museum Technical Research Bulletin*, *8*, 83–92.

WISEMAN, G., BARNES, S., & HELWIG, K. (2023). Investigation of Egyptian Blue on a Fragmentary Egyptian Head Using ER-FTIR Spectroscopy and VIL Imaging. *Heritage*, *6*, 993–1006. ↗.